JET TRAINER AEROFOIL SELECTION

J.Benetka, M.Kladrubský, Z.Pernica
VZLÚ(ARTI) - Aeronautical Research and Test Institute
Prague , Czechoslovakia

Abstract

The paper contains description of both theoretical and experimental methods used for preliminary selection of an aerofoil, convenient for application to a jet trainer wing of new generation. The theoretical method consists of a calculation code containing two-dimensional solution of transonic flow around an aerofoil and employs viscid/inviscid interaction of full-potential equation and three-component boundary layer (laminar - forced or free transition including laminar separation buble - turbulent) . The experimental method comprises pressure measurements of the aerofoils in two-dimensional test section of slotted walls, to which an empirical method of wall corrections was applied.

Both methods were compared and indicated limiting properties of the aerofoils such as values of drag, maximum lift , Mach number of drag divergence, pitching moment e.t.c.

I. Introduction

The article illustrates a procedure , used to select a basic wing aerofoil of a new generation jet trainer supposed to be of maximum take-off mass of approximately 5000 kg. The selection is based on a comparative study of aerodynamic characteristics of aerofoils designed for the supposed application . To keep a reasonable extension of the article two of these aerofoils are introduced only , i.e. AS 12/27 and AS 12/28 (1). Their characteristics are related to those of aerofoil NACA 64A012mod.5 used at the wing of the previous generation jet trainer AERO L-39 Albatros , which can be used as a reference base enabling one to judge improvements reached by newly designed aerofoils. An opposite reference margin of the aerofoils group forms MS(1)-0313 , whose low-speed characteristics were published for a range of Reynolds numbers (2), and which limits this group namely by its high pitch moment and high design lift coefficient.

The aerodynamic characteristics of these aerofoils were obtained by two ways : experimentaly by measurement in transonic wind tunnel , Reynolds number of experiments being max. 2.2 x 10^6 and by theoretical calculations for tunnel and flight Reynolds numbers.

The development of military trainers in recent years has led to appearence of a variety of aircraft of different power units, flight speeds and masses . The choise of the type depends particularly on the pilot training conception in which the economy plays an evergrowing role. The pilot trai - ning conception then finds a reflection in technical limitations for a new trainer development and through it in technical conditions for a lift system design and consequently for an aerofoil design.

Authors are well aware that shaping the wing as a whole is a fundamental task in achieving economical production and operation of an aircraft and its good performance and properties . This task requires a three-dimensional solution , which cannot be understood as a simple extension of a two - dimensional solution . Nevertheless they still remain convinced in the usefulness of two-dimensional study of aerofoils, which may be a good basis for wing design particularly for a trainer which is specific by its very wide spectrum of flight regimes. A comparison of a variety of different aerofoils over all their off-design working field helps to discover weak spots or to find out their advantages . It seems that such a comparative study cannot be replaced by any design procedure , even not by an optimization.

II. Aerofoils comparision criteria

The aerofoils comparision is to evaluate their properties from point of view of their design acceptability , manufacture simplicity , operation economy and as good as possible flight performance and properties.

The design acceptability of an aerofoil is given by its convenient shape and thickness including the shape and thickness of its trailing edge , namely owing to the solution of the wing flaps . Leading - edge flaps are not usual with the trainer wing. An optimum of aerofoil thickness seems to be about 12 per cent both from the point of view of mass/load ratio and c_{Lmax}/gliding quality . The design acceptability solves essentially the manufacture simplicity, too.

The operation economy in most regimes is effected by drag . A multiregime aircraft

which the jet trainer is , requires low drag for both $c_L \sim 0.3$ when $M_\infty \sim 0.4$, corresponding to a horizontal flight , and for $c_L \sim 0.4$ when $M_\infty \sim 0.7$, corresponding to a sustained turn of load factor $n = 4g$. The second requirement can be met only when almost isentropic transonic recompression on the upper aerofoil surface is realized . Beside the low drag values the gradient dc_D/dc_L is required to be as low as possible . Also a low pitching moment has to be introduced in connection with the economy , reducing both mass of wing and the induced drag. A high drag divergence Mach number M_{DD} contributes favourably to the whole pilot training economy enabling him to widen the flight envelope and in this way to perform a part of combat missions which would otherwise have to be trained on military aircraft only. Beside the high M_{DD} a favourable change of it with c_L in the full range of the load factor is required.

As convenient flight performance one may consider those which support the economy of training. Generally , besides the low c_D and high M_{DD} already introduced, one can mention a high lift/drag ratio and c_{Lmax} as high as possible.

Characteristics favourably affecting flight properties are as follows:

- stall occurs at a high angle of attack

- separation at stall starts from the trailing edge and propagates gradually upstream

- course of all the aerodynamic characteristics is as smooth as possible within critical regimes range, i.e. at stall and entrance to transonic flight ; this includes no drag creep

- sufficient clearance of transonic buffet M_{buf} from M_{DD} , desirable value being 0.1
- good properties at flying on back.

III. Experimental equipment and method

The experimental data of all the aerofoils compared were obtained in VZLÚ transonic wind tunnel[3] of 0.8 m x 0.4 m test section . The tunnel is of vacuum type with interrupted action , operating with the atmospheric air . This causes a strong dependence of Reynolds number on the stream Mach number for a given model. In the tests presented the Reynolds number varied between $0.5 * 10^6$ at $M_\infty = 0.15$ and $2.2 * 10^6$ at $M_\infty = 0.92$ based on the model chord 0.15 m .

The floor and ceiling of the tunnel test section were slotted. The four slots are of variable open-area ratio from 0 to 10 per cent, which can be moreover linearly varied along the tunnel axis to minimize blockage effect. Neverthless an interference correction procedure was attempted.

The lift and pitching moment were obtained by an integration of pressure distribution measurement at 48 static holes spread across the middle part of the model, spanning 400 mm between sidewall windows . The holes centreline was deflected 15 degrees from the test section plane of symmetry. The profile drag was obtained from wake total and static pressure measurement, performed by a rack probe of 103 Pitot tubes situated in the probe middle part in three rows to ensure sufficiently dense pressure sampling [4].
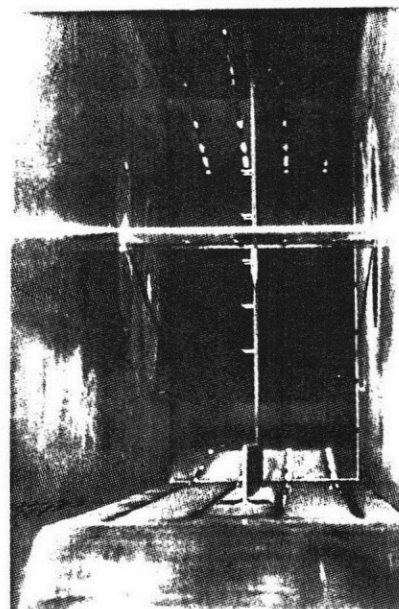

Fig.1: Test Section Internal View

The pressures were led through 16 scanning valves to pressure transducers analogical signals of which were sampled and processed to give semi-real-time results . The accuracy of the measurements was limited by an actually non-stationary nature of flow , namely in transonic regimes , requiring the integration time long enough to enable collecting sufficient quantity of samples.

The interference corrections were applied to the measured results in subsonic region. When slots were opened by 6 per cent , the blockage of the stream caused by the slotted walls was neglected as well. The only correction cosidered was the effect of inclination of the stream behind the aerofoil , thus changing the actual aerofoil angle of attack. It was found that the correction formula corresponding to given open-area ratio can be accepted in the form

$$\Delta \alpha = -K * \bar{\beta} * \frac{c}{H} * c_L$$

where $\bar{\beta}$ is compressibility factor. Its value for $M_\infty \leq 0.6$ is identical to the Prandtl

—Glauert factor but for higher M_∞ it falls rapidly down reaching for $M_\infty = 0.7$ a value equal to zero. The correction factor $K = 7.33$ was accepted which was obtained by the empirical procedure published[5]. The theoretical estimation of this value, done according to Barnwell et al [6], gave a value very close to the empirical one, finally accepted in the correction procedure.

A side-wall boundary layer effect was neglected, too. This decision was accepted after finding out that even more pronounced effect of side wall-aerofoil interaction are corner eddies which both displace the main stream from the walls and induce transversal velocity components namely at high angles of attack.

The serious effect, which cannot be corrected but which has to be considered when applying the tunnel results to an actual wing, is the Reynolds number because its tunnel value is by order lower as compared to flight value. To get an idea of this effect MS(1)-0313 aerofoil measurements published[2] were compared with those taken at VZLÚ. The expected differences in drag, lift/drag ratio and c_{Lmax} were found. An example of c_{Lmax} change with Re is shown in Fig.2.
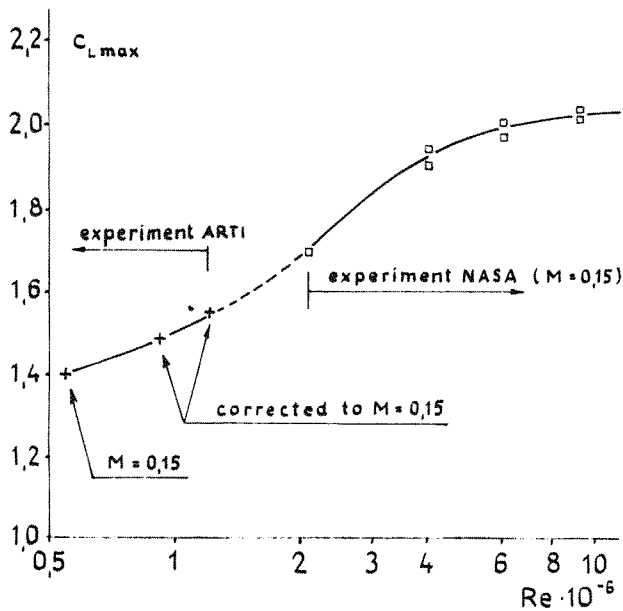

Fig.2: Change of Measured c_{Lmax} with Re

As there was no other choice, the authors decided to compare the aerofoils under study at low Re, running the risk of not fully adequate conclusions. To support validity of these conclusions for higher Re theoretical calculations described in the following chapter were used.

IV. Theoretical method

The theoretical method used employs viscid/inviscid interaction between a potential model and an integral method of boundary layer solution.

The flow field is described by a potential equation in non-conservative form solved in a curvilinear C-type grid, the transformation coefficients being determined locally during the calculation. In this grid the equation is of form

$$C_1 \phi_{\xi\xi} + C_2 \phi_{\eta\eta} + C_3 \phi_{\xi\eta} - p_x u - p_y v = 0$$

where

$$C_1 = B_{11} - \left(\frac{U}{q}\right)^2 M^2$$

$$C_2 = B_{22} - \left(\frac{V}{q}\right)^2 M^2$$

$$C_3 = 2\left(B_{12} - \frac{U V}{q^2} M^2\right)$$

$$p_x = C_1 X_{\xi\xi} + C_2 X_{\eta\eta} + C_3 X_{\xi\eta}$$

$$p_y = C_1 Y_{\xi\xi} + C_2 Y_{\eta\eta} + C_3 Y_{\xi\eta}$$

$$u = \phi_x \quad , \quad v = \phi_y$$

ϕ is the velocity potential,

U , V are proportional to contravariant velocity components in the coordinates (ξ, η).

$$\begin{Bmatrix} U \\ V \end{Bmatrix} = \{J\}^{-1} \cdot \quad \begin{Bmatrix} u \\ v \end{Bmatrix} = \{J^T J\}^{-1} \begin{Bmatrix} \phi_\xi \\ \phi_\eta \end{Bmatrix}$$

$$= \begin{Bmatrix} B_{11} & B_{12} \\ B_{12} & B_{22} \end{Bmatrix} \begin{Bmatrix} \phi_\xi \\ \phi_\eta \end{Bmatrix}$$

In a supersonic region there the Jameson s rotation scheme

$$(1 - M^2)\left[\left(\frac{U}{q}\right)^2 \overline{\phi}_{\xi\xi} + \left(\frac{V}{q}\right)^2 \overline{\phi}_{\eta\eta} + 2\frac{UV}{q^2}\overline{\phi}_{\xi\eta}\right]$$

$$+ \left[B_{11} - \left(\frac{U}{q}\right)^2\right]\phi_{\xi\xi} + \left[B_{22} - \left(\frac{V}{q}\right)^2\right]\phi_{\eta\eta}$$

$$+ 2\left[B_{12} - \frac{UV}{q^2}\right]\phi_{\xi\eta} - p_x u - p_y v = 0$$

is used, where $\overline{\phi}_{\xi\xi}$ e.t.c. are the upstream differences.

The viscous effects are included in the solution by solving integral equations of compressible boundary layer. It contains method of solution of a laminar boundary layer, transition natural (including a laminar separation bubble) or forced and a turbulent boundary layer.

For the laminar part Thwaites method is used[8]. The separation is supposed to occur when parameter

$$m = -\frac{\theta^2}{\nu_e} \frac{dU_e}{ds} \frac{T_w}{T_e} Re$$

is of value $m \gtrsim 0.09$. The transition is determined by means of Schlichting-Granville criterion [9]

$$R_{\theta inst} = R_{\theta cr}(\lambda) \; ; \; \lambda = R_\theta \frac{\theta}{U_e} \frac{dU_e}{ds} \frac{\nu_o}{\nu_e} k_{Su}$$

$$R_{\theta tr} = R_{\theta inst} + \Delta R_\theta(\bar{\lambda}) \; ; \; \bar{\lambda} = \frac{1}{s-s_{inst}} \int_{s_{inst}}^{s} \lambda \, ds$$

where k_{Su} is coefficient in Sutherland's viscosity-temperature relation.

At the transition point it holds good that

$$H_T = H_L - \Delta H(R_\theta)$$

The length of the transition region is

$$s_T - s_{tr} = Re_{\Delta s} \frac{\nu_e}{u_e} \; ; \; Re_{\Delta s} = f(M_e, Re_{s \, tr})$$

Within the region $s \in (s_{tr}, s_T)$ there is

$$\delta = (1 - \gamma) \delta_L + \gamma \delta_T$$

where γ is an increasing function between values

$$\gamma = 0 \quad at \quad s = s_{tr}$$
$$\gamma = 1 \quad at \quad s = s_T$$

In the case of laminar separation then a transition in bubble is tested according to Horton[10]

$$l_{sep} = \frac{5 \ast 10^4 \, \theta_{sep}}{R_{\theta sep}} \qquad \theta_R = \theta_{sep} \left(\frac{U_{esep}}{U_{e \, R}} \right)^3$$

The turbulent boundary layer is solved by the lag-entrainment method of Green et al[11].

Starting conditions for the turbulent boundary layer were as follows

$$C_E = (C_E)_{EQo} \quad \text{(values of } H \text{ and } \theta \text{ being known)}$$

at transition of adjacent stream and

$$c_f = c_{fo} = 0$$

$$\bar{H} = 2.2 \, \bar{H}_o \qquad C_E = 2 (C_E)_{eyo}$$

behind the laminar separation bubble[12].

The viscous effects are included in the non-viscous scheme by means of non-zero normal velocity component on aerofoil surface and in the wake.[13]

The transpiration velocity can be deter-

mined from boundary layer solution as follows:

$$\sigma = v_n / q$$

$$v_n = \frac{1}{\rho} \frac{d}{ds}(\rho \, q \, \delta^*) = \frac{d\delta^*}{ds} + (1 - M_e^2) \frac{\delta^*}{q} \frac{dq}{ds}$$

On the aerofoil surface in transformed coordinates this condition takes a form

$$(v/q)/\sqrt{B_{22}} = \sigma$$

Along the wake its thickness change caused by the boundary layer is considered only while its curvature change is neglected. Thus the boundary condition along the wake is

$$\frac{\Delta v_n}{q} = \frac{1}{q\rho} \frac{d}{ds}(\rho \, q \, \delta^*)$$

where

$$\Delta v_n = v_n^+ - v_n^- \quad , \quad \delta^* = \delta^{*+} - \delta^{*-}$$

$+(-)$ denotes upper(lower) side of the wake. Expressed in calculation coordinates it holds good that

$$\frac{1}{q\sqrt{B_{22}}}(v^+ - v^-) = \sigma^+ + \sigma^-$$

This approach employs direct solution of boundary layer and thus it is very sensitive to change of boundary layer displacement thickness, particularly close to the trailing edge. To obtain a next-step displacement thickness the under - relaxation is used

$$\delta^* = \omega (\delta^*_{new} - \delta^*_{old}) + \delta^*_{old}$$

where parameter ω is selected in range of $0.05 - 0.15$ according to the ratio $\delta^*_{TE \, old} / \delta^*_{TE \, new}$.

AS 12/27   MACH   HE   AL
THEORY VPT ———— .753   2.02E6   0.0
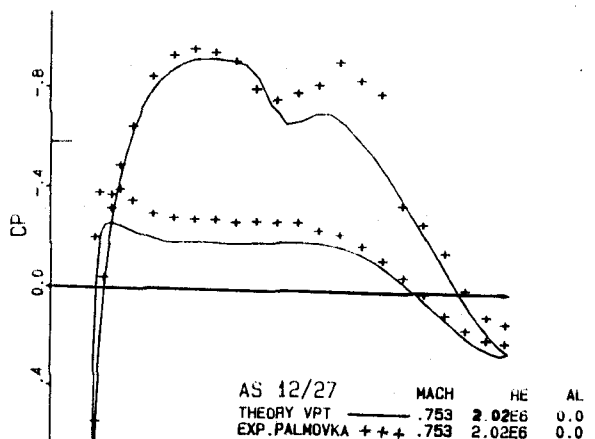EXP.PALMOVKA +++ .753   2.02E6   0.0

Fig.3: Comparison of calculation and measurement of c_p on AS 12/27

V. Comparative study

The aerofoils under study are in Fig.4 where their shapes and c_p distributions for $c_L \sim 0.3$ at $M_\infty = 0.4$ are introduced.
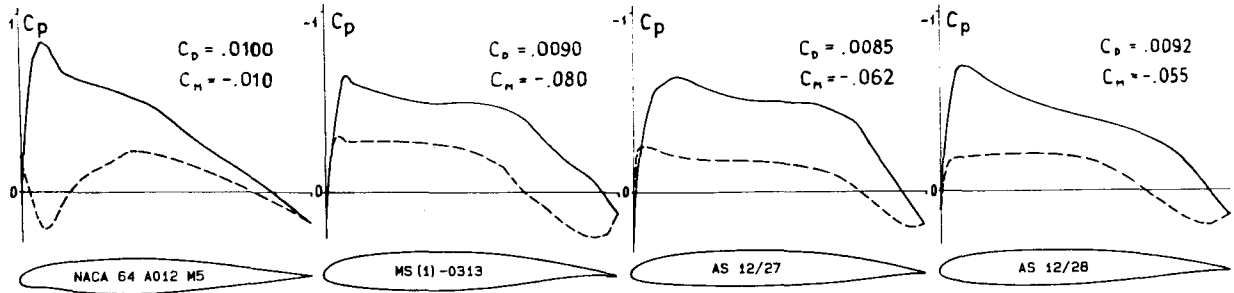
The aerofoils work at this regime mostly under a negative angle of attack and their lower front parts are in supercritical flow. As the drag coefficients indicate AS 12/27 appears to be the best for $M_\infty = 0.4$ whereas AS 12/28 for $M_\infty = 0.7$. As regards their moments, both reference aerofoils form two limits, between which are moments of the new aerofoils. Among them AS 12/28

$C_D = .0100$ $C_M = -.010$ NACA 64 A012 M5

$C_D = .0090$ $C_M = -.080$ MS (1) -0313

$C_D = .0085$ $C_M = -.062$ AS 12/27

$C_D = .0092$ $C_M = -.055$ AS 12/28

Fig.4: Shapes and c_p distributions of the aerofoils at $M_\infty = 0.4$ and $c_L \sim 0.3$

As it has been already stated, this regime corresponds to the cruise horizontal flight. In an attempt to qualify the pressure distributions it can be said that NACA 64A012mod.5 is characterized by its front part load, while MS(1)-0313 keeps almost constant load till 95 per cent of its chord. The aerofoil AS 12/27 shows nearly constant load except its rear quarter of chord, where the load is gradually reduced. AS 12/28 features more loaded front part, less loaded rear one with the minimum in the middle. Both of these load types aimed to reduce somewhat the pitching moment, AS 12/28 is moreover an alternative for improved behaviour in transonic regimes. It can be seen from Fig.5 that the nature of the load changes with increasing flight velocity.

provides more convenient course with M_∞, as it is demonstrated in Fig.6.

AS 12/27
AS 12/28 ∇ M_{DD}
NACA $*$ CR L lower surface
                     U upper surface
MS(1)-0313 o $C_{pTE} = 0$
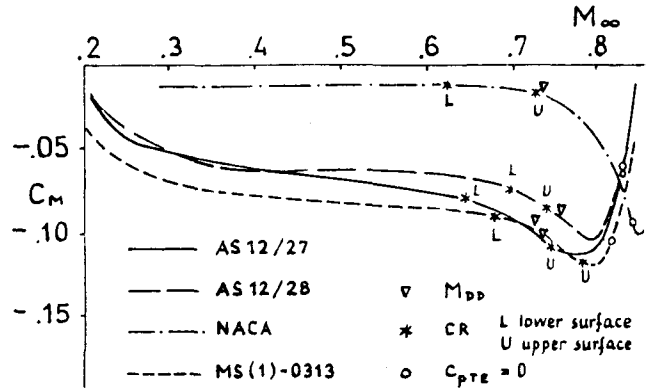
Fig.6: Course of pitching moments with M for horizontal flight

The following comparative study can be undertaken as a real choice of convenient aerofoil for a jet trainer but the explanation of behaviour of various load type aerofoils at off-design conditions is more valuable. Basic characteristics used for this study were those introduced in Fig.7, i.e. $c_L = c_L(\alpha, M_\infty)$, which are shown only for aerofoils NACA 64A012mod.5 and AS12/27. Beside the lift curves, M_{DD} limits, lines of sonic critical regimes for upper and lower surfaces and separation boundaries defined by c_p on the trailing edge $c_{pTE} = 0$ are drawn. The characteristics are completed by two lines of aircraft operation regimes, for steady horizontal flight at $H = 5km$ and for sustained turn with the load factor $n = 4g$ in the same altitude.

The superiority of the new aerofoils is obvious. Its flight envelope is clearly wider in both M_∞ and c_L directions, parti-

$C_D = .0120$ $C_M = -.015$ NACA 64 A012 M5

$C_D = -.0102$ $C_M = -.095$ MS (1) -0313

$C_D = -.0100$ $C_M = -.095$ AS 12/27

$C_D = -.0092$ $C_M = -.073$ AS 12/28

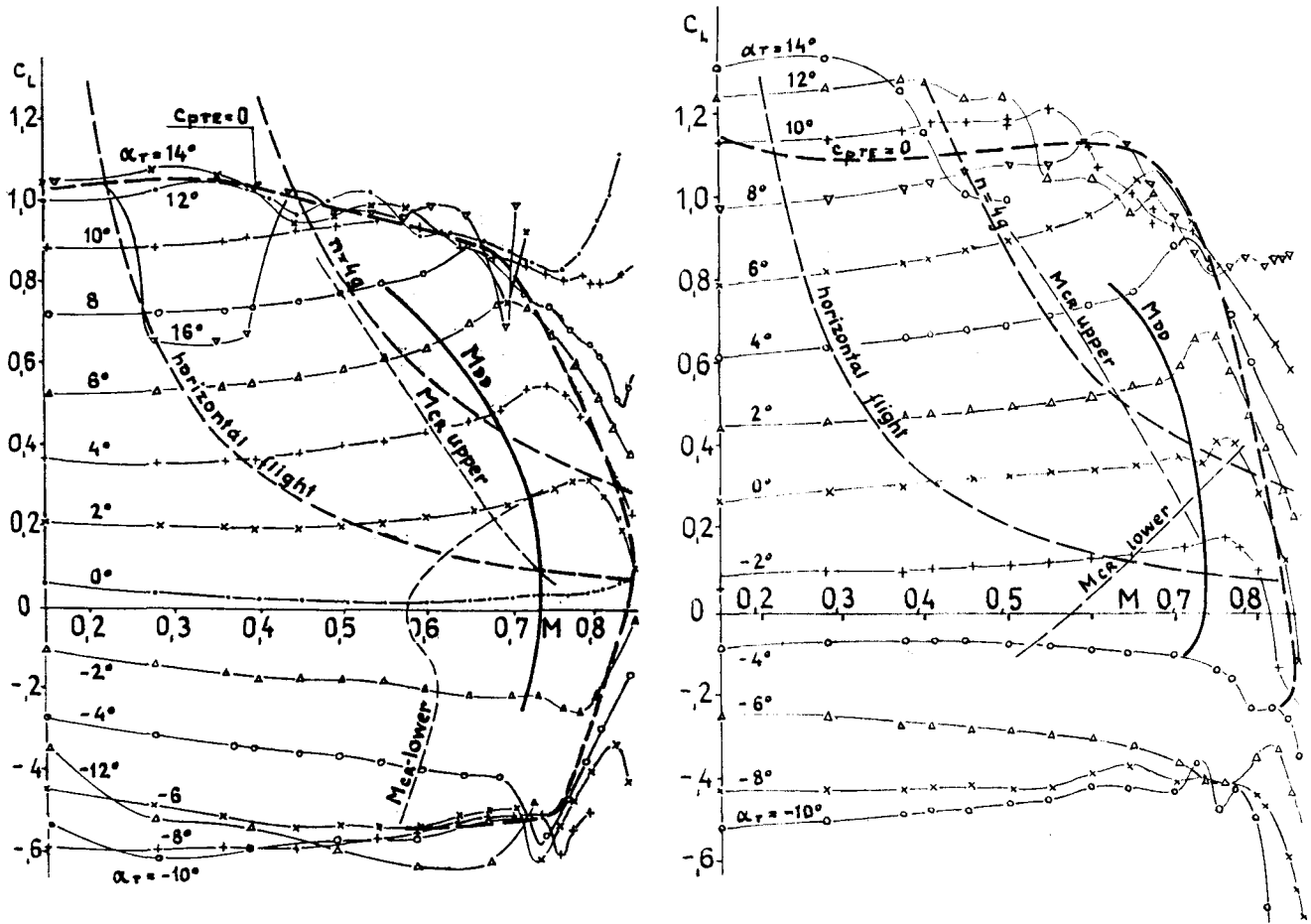Fig.5: Distribution of c_p for $M_\infty = 0.7$ and $c_L \sim 0.1$

Fig.7: Measured operation characteristics of aerofoils
NACA 64A012 mod.5   and   AS 12/27.

cularly in the "transonic corner ",which is however somewhat beyond the scope of practical interest .But interesting compa - rison can be made for sustained turn at high velocities . The reference aerofoil NACA 64A012 mod.5 operates in this region in supercritical regimes and moreover the regime $M_{\infty} = 0.7$ and $c_L = 0.4$ is already close to M_{DD} . The pressure distribution for all four aerofoils is introduced in Fig.8.

Characteristics of aerofoils load at this regime somewhat resemble those in Fig.4. The differences are of course in va- lues of c_p, the front parts are in transo - nic stream but none of the aerofoils dis- plays a separation . Among them the classi- cal aerofoil NACA shows the steepest re - compression on its upper surface and the most complicated course of c_p along the lower one which brought it to the boun- dary M_{DD} . Verification of this character of load for high Reynolds number, performed by calculation, did not bring a new piece of knowledge as can be seen in Fig.8.

A more complex look at the aerofoils be- haviour at transonic region can be obtained from Figs.6,7 and 9. None of the aerofoils
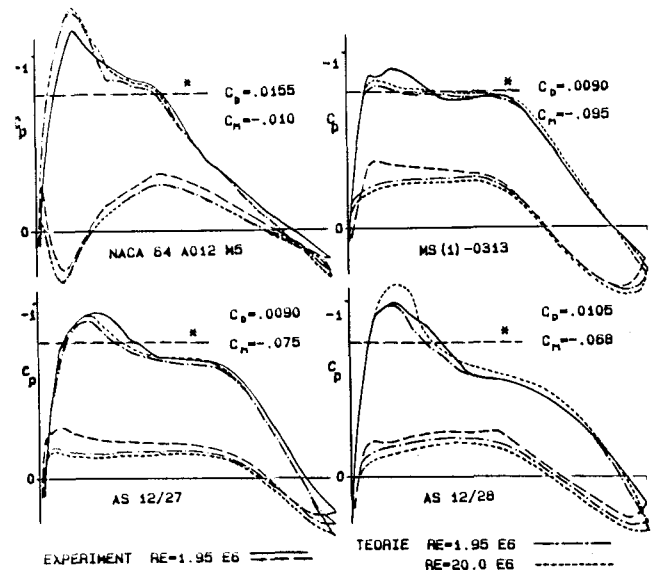

Fig.8: Pressure distribution for aerofoils
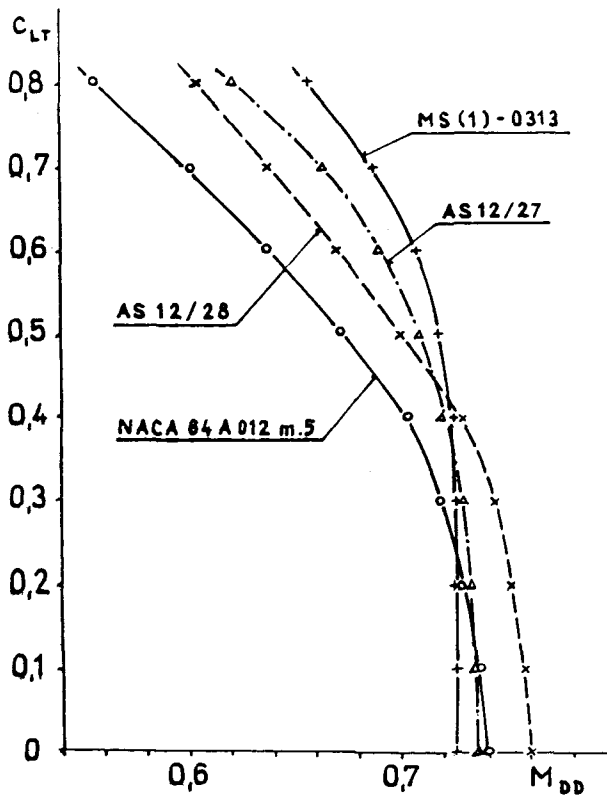at $M_{\infty} = 0.7$ and $c_L = 0.4$.

1295

Fig.9: Measured M_{DD} boundaries

Fig.10: Maximum lift coefficients c_{Lmax} versus M_∞ measured in tunnel

Fig.11: Lift, drag and moment curves of AS 12/27 at M_∞ = 0.15

Fig.12: Lift, drag and moment curves of AS 12/28 at M_∞ = 0.15

shows dramatic changes in lift and moment coefficients in the vicinity of M_{DD} . Fig.9 proves predominance of AS 12/28 regarding value of M_{DD} at low lift , criterion of M_{DD} being $dc_D / dM_\infty = 0.1$. Behind M_{DD} all the aerofoils are losing lift first and only later reach a separation characterized by $c_{pTE} = 0$. From this point of view the classical aerofoil appears surprisingly as the best one . Unfortunately validity of these facts at high Re couldn't be verified.

Another critical region of the aerofoils work falls to high lift regimes, limited by the load factor n = 4g to Mach numbers $M_\infty \leqslant 0.4$ (see Fig.7).

Measured values of c_{Lmax} for variable M_∞ are in Fig.10 . From it the advantages of the new aerofoils concept are clear .One may presume from it as well a superiority of AS 12/28 over AS 12/27 because of its somewhat higher c_{Lmax} at $M_\infty \sim 0.4$. Let us make a more detailed analysis of behaviour of these aerofoils in the vicinity of c_{Lmax}. Their lift and moment curves for low speed are in Figs. 11 and 12. They show very steep fall of c_L of AS 12/28 compared with relatively graduate decline of c_L of the aerofoil AS 12/27. This difference reflects in changes of c_M with c_L , too. A reason of this behaviour becomes clear after follow - ing c_p evolution in the vicinity of c_{Lmax} , shown in Figs. 13 and 14 . The AS 12/28 is able to sustain only a short region of se -
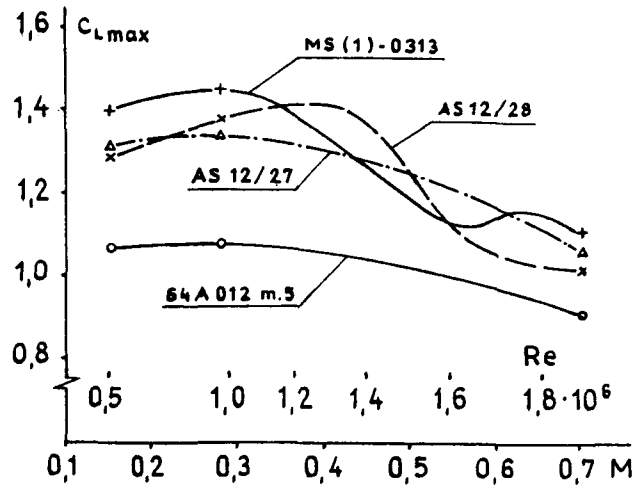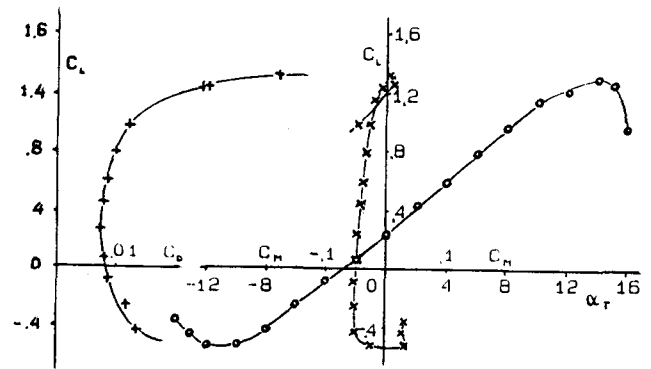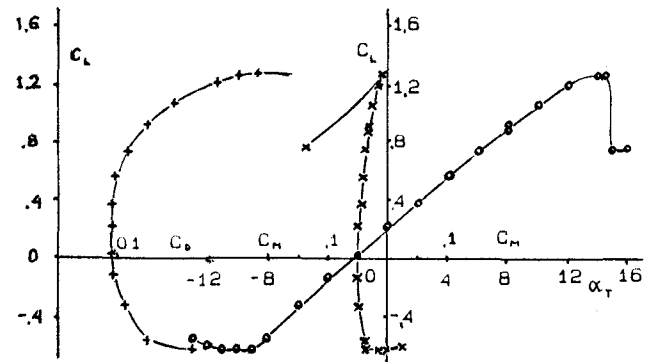
paration close to the trailing edge ($\alpha = 14.5°$). Then a small increase in inci- dence causes an abrupt shooting of the se- paration toward the leading edge . On the
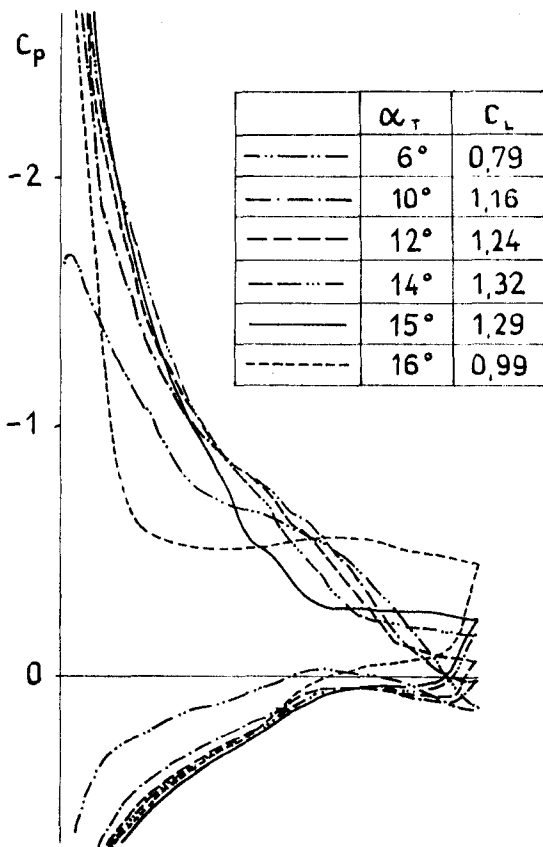
C_p

	α_T	C_L
—··—··—	6°	0,79
—·—·—	10°	1,16
— — —	12°	1,24
—···—···—	14°	1,32
———	15°	1,29
--------	16°	0,99

-2

-1

0

C_p

	α_T	C_L
—··—··—	6°	0,74
—·—·—	8°	0,92
— — —	12°	1,20
———	14,5°	1,27
--------	15°	0,76

-2

-1

0

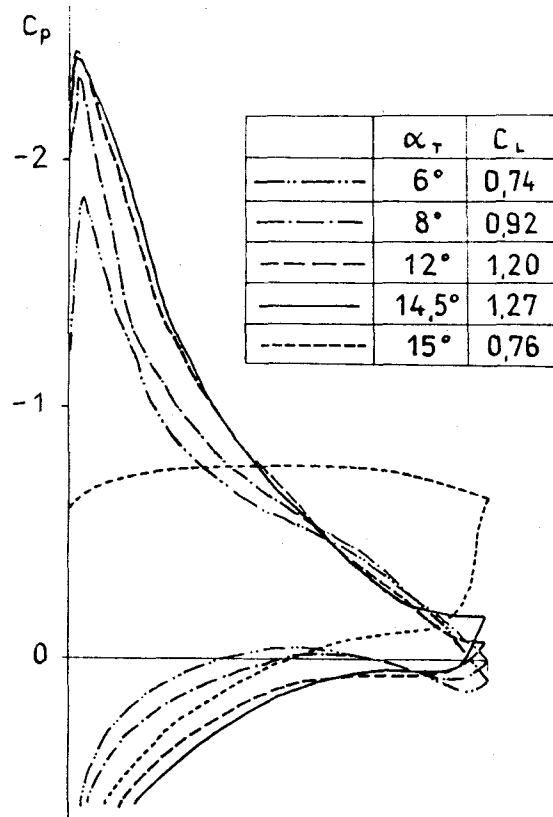Fig.13: Development of c_p on AS 12/27 with increasing α at $M_\infty = 0,15$

Fig.14: Development of c_p on AS 12/28 with increasing α at $M_\infty = 0,15$

other side the region of separation on AS 12/27 progresses from trailing to leading edge gradually and the suction peak close to the leading edge is still retained even when the aerofoil lift coefficient has declined down . Thus this aerofoil offers more chance to preserve such favourable behaviour of a wing than AS 12/28 does.

When comparing properties of these two aerofoils close to their maximum lift for negative angles of attack we have to note that AS 12/28 shows to be more resistant against the negative stall.

Between these critical regions (M_{DD} and c_{Lmax}) there is a variety of regimes in which the aerofoils are to work . Let us complement the results introduced above by additional characteristics of aerofoils, important in this middle "ordinary" region. The basic drags of the aerofoils have been already compared . In Fig.15 there are measured maximum lift/drag ratios against M_∞ . The predominance of AS12/27 is clear. Theoretical calculations and experience with another aerofoils have shown that the values of lift/dgar ratio for flight Reynolds numbers are much higher than the values measured in our wind tunnel. This increase was found to be about 60 per
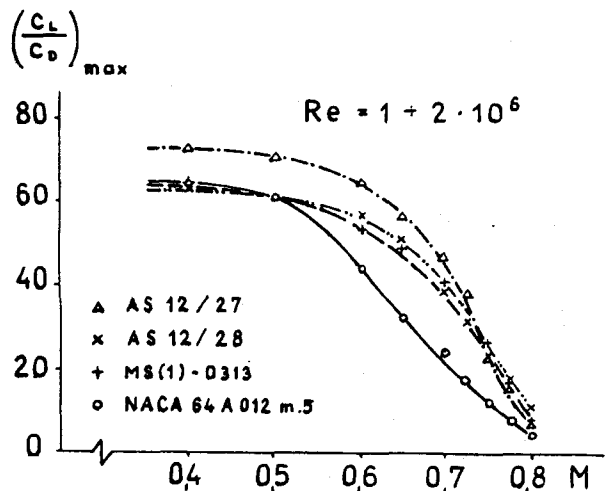
$\left(\dfrac{c_L}{c_D}\right)_{max}$

80

60

40

$Re = 1 \div 2 \cdot 10^6$

▲ AS 12/27
✕ AS 12/28
+ MS(1)-0313
○ NACA 64A012 m.5

20

0

0,4   0,5   0,6   0,7   0,8   M

Fig.15: Measured $(c_L/c_D)_{max}$ ratios for all tested aerofoils

cent or even more.

VI. Conclusions

The article presents results of a comparative study which indicated some advantages of different types of pressure distributions of aerofoils at various regimes of operation. Despite the experience that an aerofoil of high c_{Lmax} requires diffe - rent design c_p distribution than another intended for high M_{DD} and good transonic behaviour, it was shown that both of these contradictory requirements can be satisfied in some way and it is worth searching for an optimum solution. In spite of the fact that this study was performed experimentally at low Reynolds numbers and supported only by calculations at higher Re , it is believed that this general result is true.

Thus the obtained knowledge of convenient pressure distribution may become a clue to a solution of a three-dimensional wing design.

References

1. Brož, V., Slavík, S.: Design of 12 per cent supercritical aerofoils, Zpráva VZLÚ, 1987 (in Czech).

2. Mc Ghee, R.J., Beasley, W.D.: Low - Speed Aerodynamic Characteristics of a 13-Percent-Thick Medium-Speed Airfoil Designed for General Aviation Applications, NASA TP 1498, 1979.

3. Benetka, J..: Measurement of aerodynamic characteristics of 4 aerofoils at high - speed wind tunnel, Zpráva VZLÚ, 1990 (in Czech).

4. Pernica,Z., Kladrubský, M.: Comparative measurements of NACA 64A012 mod.5 and a supercritical aerofoil at high speeds, Zpráva VZLÚ V-1468/82, 1980 (in Czech).

5. Dixon, R.C.: High Reynolds Number Investigation of an ONERA Model of the NACA 0012 Airfoil Section, NAE Report LTR-HA-5x5/0069, 1975.

6. Barnwell, R.W. et al : Design and Calibration of Slotted Walls for Transonic Airfoil Wind Tunnel, NASA CP 2045, 1978.

7. Chen, L.T., Caughey, D.A.: Calculation of Transonic Inlet Flowfields Using Generalized Coordinates, J.Aircraft, Vol.17, No.3, March 1980.

8. Curle, N.: The Laminar Boundary Layer Equations, Oxford University Press, 1962.

9. Mc Nally, W.D.: Fortran Program for Calculating Ccmpressible Laminar and Turbulent Boundary Layers in Arbitrary Pressure Gradients, NASA TN D-5681, 1970.

10. Roberts, W.B.: Calculation of laminar separation bubbles and their effect on airfoil performance, AIAA Journal, Vol.18, No.1, 1980.

11. Green,J.E., Weeks,D.J., Brooman,J.W.F.: Prediction of Turbulent Boundary Layers and Wakes in Compressible Flow by a Lag Entrainment Method, A.R.C. R M 3791, 1973.

12. Příhoda, J.: Transition of Boundary Layer and its Calculation, Zpráva ČSAV Z-979/86, 1986.

13. Lock, R.C., Firmin, M.C.P.: Survey of Techniques of Estimating Viscous Effects in External Aerodynamics, Proc. IMA Conference on Numerical Methods in Aeronautical Fluid Dynamics, Reading , 1980.